

Response of strongly coupled fermions on classical and quantum computers

John Novak¹, Manqoba Q. Hlatshwayo², and Elena Litvinova^{1,3*}

¹ *Department of Physics, Western Michigan University, Kalamazoo, MI, 49008, USA*

² *National Quantum Computing Centre, Didcot, OX110QX, United Kingdom*

³ *Facility for Rare Isotope Beams, Michigan State University, East Lansing, MI, 48824, USA*

(Dated: May 6, 2024)

Studying the response of quantum systems is essential for gaining deeper insights into the fundamental nature of matter and its behavior in diverse physical contexts. Computation of nuclear response is critical for many applications, but its spectroscopically accurate description in medium-heavy nuclei in wide energy ranges remains particularly challenging because of the complex nature of nuclear quantum states in the high-level-density regime. Herein, we push the limits of configuration complexity in the classical computation of the nuclear response and present an algorithm with a quantum benefit for treating complex configurations. The classical computational method of approaching spectroscopic accuracy is implemented for medium-heavy nuclei and pioneered for the dipole response of ¹²⁰Sn, while the quantum algorithm reaching the exact solution is realized for the Lipkin Hamiltonian to unravel the emergence of collectivity at strong coupling.

Probing strongly interacting quantum systems reveals a rich interplay of fundamental interactions, quantum entanglement, many-body effects, and phase transitions. Modeling atomic nuclei and nuclear matter of neutron stars, in particular, relies on knowledge about nuclear compressibility, polarizability, and various decays, which is critical for many applications. The nuclear response, the major source of this information, is especially challenging because its accurate computation requires thorough knowledge of nucleon-nucleon interaction in the low-energy limit of quantum chromodynamics and non-perturbative solutions for the many-body problem of strongly coupled self-bound nucleons.

The response of interacting fermionic systems can be quantified by the equation of motion (EOM) for the propagation of a pair of fermions through the correlated medium. This equation is, in principle, exact [1–4]; however, its integral part is connected with the hierarchy of the higher-rank propagators, making the exact solution intractable for heavy nuclei. Reasonable approximations are possible to decouple the interaction kernel from this hierarchy while keeping the leading effects of emergent collectivity [1, 5, 6]. The formation of collective degrees of freedom appears in many nuclear structure contexts. The most evident signatures of collectivity are (i) the inability to interpret the large probabilities of transitions to some excited (collective) states in terms of the pure single-particle motion and (ii) superfluidity manifested in the nuclear rotations and spectral gaps [7]. The exact response EOM formulated in the space of the Bogoliubov quasiparticles [8] takes collectivity and superfluidity into account on equal footing, thus setting a rigorous microscopic framework for controllable approximations to the response of strongly interacting fermionic systems.

Early approaches to the nuclear response employed phenomenological effective forces and empirical couplings between the single-particle and collective modes. Nuclear

field theory (NFT) [9–13], quasiparticle-phonon model (QPM) [14, 15] and extensions of the Landau-Migdal theory [16, 17] were particularly advanced in the description of fragmentation mechanisms with the minimal (quasi)particle-vibration coupling ((q)PVC). With the advent of accurate nuclear energy density functionals (EDF), self-consistent qPVC approaches became available [18–23]. However, although the leading-order qPVC enabled a reasonable description of the gross properties of the nuclear response, it is still insufficient for spectroscopically accurate results demanded by nuclear data, stellar astrophysics, and new physics searches at the precision frontier.

The recent effort was dedicated to the refined computation of the nuclear response. Bare nucleon-nucleon interactions were employed [24–26] and higher configuration complexities were explored [27–31] in the studies of medium-heavy nuclei, which indicated that complex configurations are responsible for fine spectral details. Combining the ab-initio EOM [3, 4, 6] and effective meson-exchange nucleon-nucleon interaction [32–34], the relativistic NFT (RNFT) introduced self-consistent computation of the response of medium-light nuclei with correlated three-particle-three-hole (*3p3h*), or six-quasiparticle (*6q*) configurations [8, 35] organized by qPVC, in the wave functions of the excited states. These studies revealed that (i) this configuration complexity is necessary for achieving spectroscopic accuracy, and (ii) the results may saturate quite fast with configuration complexity. We hypothesize that the latter can thus reliably serve for the uncertainty quantification of the many-body method when applied also to heavier nuclei and, further, to fermionic systems with arbitrarily strong coupling.

In this work, we formulate an approach for the fermionic response with a variable configuration complexity and demonstrate its validity in two contexts. First, the RNFT implementation of the *6q* configuration complexity is advanced to considerably larger model space and pioneered for medium-heavy superfluid tin nuclei

* elena.litvinova@wmich.edu

in classical computation. Second, we tackle the problem with the quantum EOM (qEOM) algorithm, originally proposed for calculations of energy eigenstates of fermionic systems [36] and later to the single-fermion Green functions [37]. Here, we promote the qEOM to the quantum computation of the response function and discover its quantum benefit in treating complex configurations at strong coupling for the response of the Lipkin-Meshkov-Glick (LMG) Hamiltonian [38]. Although LMG is a generic testbed for many-body physics [39–41] and quantum algorithms [42–47] because of its scalable coupling and integrability, its response properties were largely unknown. Our LMG study reveals the role of complex configurations in the LMG response and tracks the emergence of collectivity over the coupling regimes with quantified uncertainties.

In the field-theoretical formalism widely applicable across the energy scales from particle physics [48] to quantum chemistry [5], the response of a fermionic system to a local external operator is associated with the two-time correlation function defining in-medium particle-hole (two-quasiparticle) propagation:

$$R_{ij,kl}(t-t') = -i\langle T\psi_i^\dagger(t)\psi_j(t)\psi_i^\dagger(t')\psi_k(t') \rangle, \quad (1)$$

where $\langle T\dots \rangle$ stands for the chronologically ordered expectation value in the ground state and $\psi_i(t)$, $\psi_i^\dagger(t)$ are the fermionic field operators in the Heisenberg picture at time t . The Latin subscripts stand for the single-particle basis states, and in the covariant formulation, the Hermitian adjoints are replaced by the Dirac adjoints. The response function contains the entire spectrum of excited states $|n\rangle$, which is commonly accessed via its Fourier transform

$$R_{ij,kl}(\omega) = \sum_{n>0} \left[\frac{\rho_{ji}^n \rho_{lk}^{n*}}{\omega - \omega_n + i\delta} - \frac{\rho_{ij}^{n*} \rho_{kl}^n}{\omega + \omega_n - i\delta} \right], \quad (2)$$

where the poles ω_n are the excitation energies above the ground state $|0\rangle$, $\delta \rightarrow +0$, and $\rho_{ij}^n = \langle 0|\psi_j^\dagger\psi_i|n\rangle$ are the transition densities. The EOM for the response function is the Bethe-Salpeter-Dyson equation (BSDE), whose operator form reads:

$$R(\omega) = R^{(0)}(\omega) + R^{(0)}(\omega)K[\rho^{(2)}, R^{(4)}(\omega)]R(\omega), \quad (3)$$

with $R^{(0)}(\omega)$ being the uncorrelated particle-hole propagator and $K(\omega)$ the complete interaction kernel. In this formulation, the kernel $K(\omega)$ plays the role of the in-medium interaction between the fermions. Its schematic form is displayed in Fig. 1(a), omitting technical details available in Refs. [6, 8]. The essential feature of $K(\omega)$ is its decomposition into the static and dynamic components, where the former consists of the bare (antisymmetrized two-body) fermionic interaction \bar{v} contracted with the correlated two-fermion density $\rho_{ijkl}^{(2)} = \langle \psi_k^\dagger\psi_l^\dagger\psi_j\psi_i \rangle$ and the latter comprises the two-time four-fermion correlation function $R_{ijkl,mnpq}^{(4)}(t-t') =$

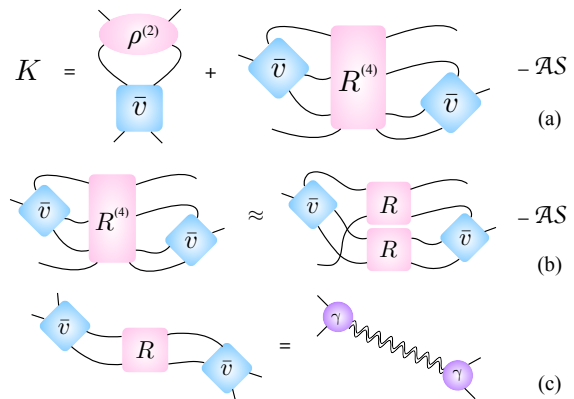


FIG. 1: Schematic exact interaction kernel (a), its approximation truncated at the two-body level (b), and the emergence of collective degrees of freedom (c). The symbol \bar{v} denotes the antisymmetrized bare interaction, $\rho^{(2)}$ is the two-body density, and $R^{(4)}$ is the propagator of four quasiparticles. Connecting solid lines are assigned to quasiparticles (particles and holes), and the wiggly line denotes the phonon propagator. 'AS' stands for omitted terms with antisymmetrized fermionic operators [6, 8].

$-i\langle T(\psi_i^\dagger\psi_j^\dagger\psi_k\psi_l)(t)(\psi_p^\dagger\psi_q^\dagger\psi_n\psi_m)(t') \rangle$ contracted with two matrix elements of \bar{v} .

The dynamic component represents the long-range correlations associated with the system size because of the presence of the propagator $R^{(4)}(t-t')$, while the static one is practically instantaneous, having nearly the range of the bare interaction. Since $R^{(4)}$ further couples to higher-rank propagators $R^{(k)}$ with $k > 4$, reasonable approximations are needed to make the EOM (3) tractable. The cluster decomposition $R^{(4)} \sim R \otimes R$ illustrated schematically in Fig. 1(b) is of particular interest for nuclear systems as it enables a closed form of the BSDE with respect to the correlation function R and keeps important effects of the emergent collectivity. The latter is featured in Fig. 1(c) as one correlation function R in the factorized kernel appearing in a double contraction with \bar{v} . The spectral expansion of R (2) comprises poles with factorized residues so that each contraction results in a vertex function $\gamma_{ij}^n = \sum_{kl} \bar{v}_{ijkl} \rho_{lk}^n$. The corresponding pole ω_n is the energy of the quasibound two-quasiparticle state (frequency of the vibrational eigenmode). The formed composite bosons (phonons) live in the correlated medium and play the role of mediators of the induced interaction. This mechanism expresses the emergence of the qPVC scale in fermionic systems with strong coupling, which is derivable from the underlying bare forces. In the strong coupling regime of nuclear physics, the emergent phonons are enhanced by the coherent contribution of many quasiparticle pairs so that they indeed form collective degrees of freedom, which are manifest on-shell as collective excitations.

The giant dipole resonance (GDR) is one such mode dominating the spectra of atomic nuclei, which makes it an ideal testbed for novel theoretical approaches. Since

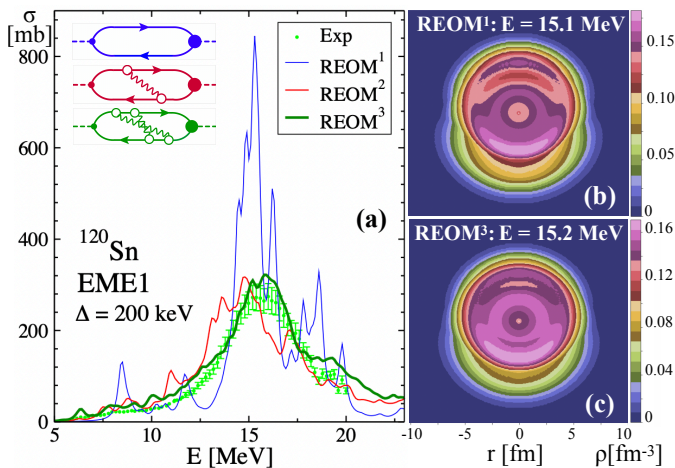


FIG. 2: Isovector giant dipole resonance in ^{120}Sn in REOM $^{1-3}$ approaches identified with the major polarization diagrams in the qPVC vertex expansion, compared to data [49] (a). The GDR density profiles in REOM 1 (b) and REOM 3 (c) at centroid energies.

the exact solution for the nuclear response is beyond reach, the best benchmark for the theory is the experimental data with the given uncertainties. For this work, we have selected the recent data of Ref. [49] for the GDR in stable tin isotopes. As the dipole spectra for these nuclei look alike, we chose to focus on the isotope ^{120}Sn with well-expressed superfluidity in its neutron subsystem. For the static EOM kernel, we employed the leading-order meson-exchange interaction parametrized within the covariant EDF [50] and corrected by subtraction, restoring the consistency of the ab initio framework [51], whereas the subleading orders are taken into account non-perturbatively by the dynamical kernel. This scheme enables entering the self-consistent cycle of BSDE where the in-medium interaction requires the knowledge of multi-fermion correlation functions. In this work, the approach to the dynamical kernel outlined in Fig. 1 was implemented with up to $6q$ configurations via iterating Eq. (BSDE), so that each iteration adds two quasiparticles ($2q$) to the configuration complexity of $R(\omega)$. The first iteration neglecting the dynamical kernel yields $2q$ configurations, which correspond to the relativistic quasiparticle random phase approximation (RQRPA) [32, 33], dubbed relativistic EOM 1 (REOM 1), and generates the phonon characteristics so that each phonon represents a correlated $2q$ configuration. The second iteration (REOM 2) produces $4q$, or $2q \otimes \text{phonon}$, configurations, and the third one (REOM 3) explicitly resolves $6q$, or $2q \otimes 2\text{phonon}$, configurations in the excited state wave functions. Since the number of excited states grows as the power of configuration complexity, progressively denser spectra (2) are generated on each iteration. Numerical details are given in Ref. [35].

The nuclear response was obtained with the dipole op-

erator for the system of N neutrons and Z protons [34]

$$F = \frac{eN}{N+Z} \sum_{a=1}^Z r_a Y_{1M}(\mathbf{r}_a) - \frac{eZ}{N+Z} \sum_{a=1}^N r_a Y_{1M}(\mathbf{r}_a) \quad (4)$$

defining the strength function $S_F(E, \Delta) = -\frac{1}{\pi} \Im \langle FR(E + i\Delta) F^\dagger \rangle$, where the imaginary part of the energy variable was taken $\Delta = 200$ keV to match the experimental resolution of the data chosen for comparison. The strength distributions in REOM $^{1-3}$ and the data of Ref. [49] are displayed in Fig. 2 (a). One can see that the $2q$ configurations of RQRPA are able to correctly capture the overall behavior of the GDR in terms of its centroid and total strength, while $2q \otimes \text{phonon}$ configurations included in REOM 2 are needed for an adequate reproduction of the spreading. However, the REOM 2 strength still shows non-observed gross structures and may underestimate the centroid. The next level of configuration complexity $2q \otimes 2\text{phonon}$ achieved in REOM 3 enables eliminating the gross structure artifacts, corrects the centroid, and produces a smooth distribution, which confidently trends towards the experimental data. Panels (b) and (c) illustrate the GDR's "tomography" via density profiles obtained from the residues of Eq. (2), establishing the relationship between strong correlations in their dynamics and geometry. Out-of-phase oscillation of the proton and neutron Fermi liquids is evident; however, in the more complete REOM 3 approach, its amplitude appears smaller while density gradients are smoother in bulk, which stems from a much richer structure and mixing of states forming the spectrum (2).

The method thus demonstrates that although $n \sim N$ configuration complexity is formally needed to solve the N -body problem exactly, in practice, even at strong coupling, a moderate complexity may be sufficient. The presented approach of cumulating it is an optimal combination of fundamentality, feasibility, and accuracy for the nuclear response. Once the importance of generating complex configurations is recognized while the required n is not known a priori, more efficient methods can be designed for strongly coupled systems. Among quantum algorithms, gradually becoming an attractive alternative for such systems [45, 52–59], the quantum EOM (qEOM) [36, 44, 47, 60] is maximally aligned with this goal. Herein, we extend qEOM to the computation of the fermionic response in a hierarchy of growing-complexity approximations.

The LMG model describes a system of N fermions constrained to two N -fold degenerate energy levels and interacting via the Hamiltonian

$$H = \epsilon J_z - \frac{V}{2} (J_+^2 + J_-^2), \quad (5)$$

$$J_z = \frac{1}{2} \sum_{m=1}^N \sum_{\sigma=\pm} \sigma \psi_{\sigma m}^\dagger \psi_{\sigma m}, \quad J_\sigma = \sum_{m=1}^N \psi_{\sigma m}^\dagger \psi_{-\sigma m}, \quad (6)$$

where the index $\sigma = \pm$ differentiates the upper and lower levels and J_z, J_σ satisfy the angular momentum commutation algebra. The interaction term associated with V

scatters two particles from the same energy level up or down coupling the states that differ by two units of the angular momentum projection. The simplicity and scalability of the interaction allow us to eliminate the uncertainties of the nuclear forces, focusing solely on the interacting many-body problem. The Hamiltonian (6) enables the encoding scheme limited by $n_q = \lfloor \log_2 \left(\frac{N}{2} + 1 \right) \rfloor$ qubits [44, 47] and efficiently handled by the variational quantum eigensolver (VQE) [61] finding the ground state $|0\rangle$. The hierarchy of approximations is constructed by applying the excitation operator

$$O_n^\dagger(\alpha_m) = \sum_{\alpha=1}^{\alpha_m} \sum_{\mu} \left[X_{\mu}^{\alpha}(n) K_{\mu}^{\alpha} - Y_{\mu}^{\alpha}(n) (K_{\mu}^{\alpha})^\dagger \right], \quad (7)$$

where $K_{\mu_1}^1 = \psi_p^\dagger \psi_h$, $K_{\mu_2}^2 = \psi_p^\dagger \psi_{p'}^\dagger \psi_{h'} \psi_h$, ... with $p(h) = \{m, +(-)\}$, generating growing-complexity excited states $|n\rangle = O_n^\dagger |0\rangle$ in terms of α particle-hole ($\alpha p\alpha h$) pairs. EOM is recast as the eigenvalue equation:

$$\begin{pmatrix} \mathcal{A} & \mathcal{B} \\ \mathcal{B}^* & \mathcal{A}^* \end{pmatrix} \begin{pmatrix} X(n) \\ Y(n) \end{pmatrix} = \omega_n \begin{pmatrix} \mathcal{C} & \mathcal{D} \\ -\mathcal{D}^* & -\mathcal{C}^* \end{pmatrix} \begin{pmatrix} X(n) \\ Y(n) \end{pmatrix}, \quad (8)$$

with $\mathcal{A}_{\mu\nu}^{(\alpha\beta)} = \langle [K_{\mu}^{\alpha\dagger}, K_{\nu}^{\beta}] \rangle$, $\mathcal{C}_{\mu\nu}^{(\alpha\beta)} = \langle [K_{\mu}^{\alpha\dagger}, K_{\nu}^{\beta}] \rangle$, $\mathcal{B}_{\mu\nu}^{(\alpha\beta)} = -\langle [K_{\mu}^{\alpha\dagger}, [H, K_{\nu}^{\beta\dagger}]] \rangle$, and $\mathcal{D}_{\mu\nu}^{(\alpha\beta)} = -\langle [K_{\mu}^{\alpha\dagger}, K_{\nu}^{\beta\dagger}] \rangle$. Eq. (8) is post-processed on a classical computer, for which powerful methods exist [8, 62, 63]. The major advantage of the qEOM algorithm is the efficient evaluation of the ground-state expectation values for the matrix elements $\mathcal{A}, \mathcal{B}, \mathcal{C}, \mathcal{D}$ [36]. They are expressed by products of Pauli gates $P_k \in \{\mathbb{I}, X, Y, Z\}$:

$$\mathcal{A} = \sum_i a_i \langle \{P_0 \otimes P_1 \otimes \dots \otimes P_{n_q}\}^i \rangle \quad (9)$$

and analogous decompositions for \mathcal{B} , \mathcal{C} , and \mathcal{D} . The number of quantum measurements $\langle P_0 \otimes P_1 \otimes \dots \otimes P_{n_q} \rangle$ is limited by n_q . Increasing the configuration complexity α needed for strong coupling increases the number of terms in the sum (9) but does not significantly affect the number of measurements. This is a spectacular quantum benefit, which further extends to the strength function. For a trial excitation operator $F = \sum_{ph} (K_{ph}^1 + K_{ph}^{1\dagger})$, it reads

$$S_F(E; \Delta) = \frac{\Delta}{\pi} \sum_n \frac{|\langle 0|F|n\rangle|^2}{(E - \omega_n)^2 + \Delta^2}, \quad (10)$$

$$\langle 0|F|n\rangle = \sum_{ph, \alpha\mu} \left(X_{\mu}^{\alpha}(n) \mathcal{M}_{ph, \mu} + Y_{\mu}^{\alpha}(n) \mathcal{M}_{ph, \mu}^* \right)$$

with $\mathcal{M}_{ph, \mu} = \mathcal{C}_{ph, \mu} + \mathcal{D}_{ph, \mu}^*$, being completely determined by the solutions of Eq. (8) and its matrix elements already measured on a quantum computer.

The strength functions for the $N = 8$ LMG model smoothed by $\Delta = 0.05\epsilon$ are displayed in Fig. 3. Panels (a)-(c) show the strength as a function of energy E/ϵ and interaction $\tilde{v} = (N-1)V/\epsilon$ for the even energy levels obtained in $\alpha_m = \{1, 2, 3\}$ approximations on a simulator.

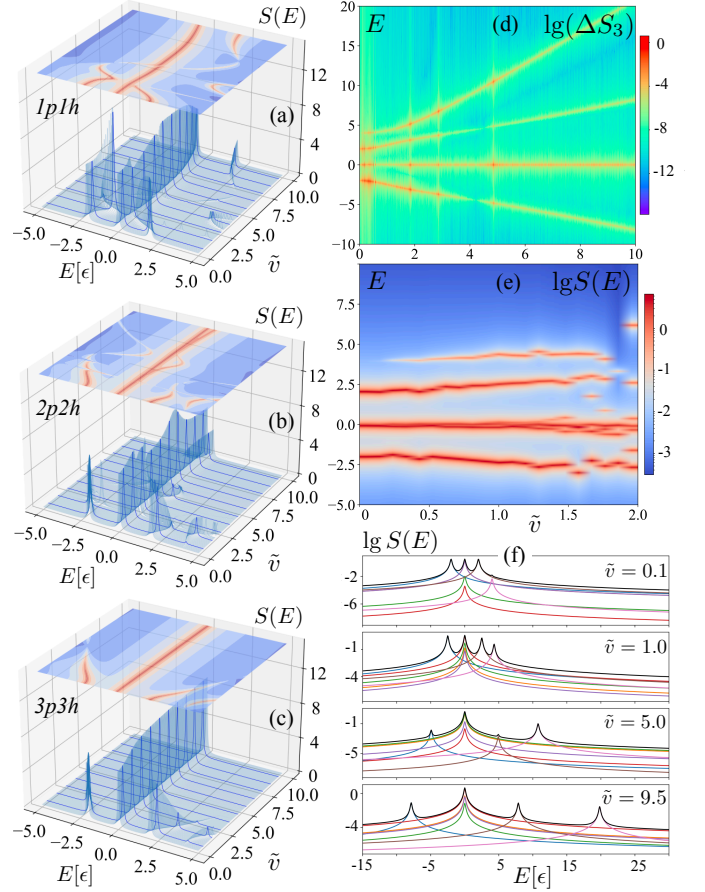


FIG. 3: Strength distributions for the LMG ($N = 8$) model obtained on a digital simulator for increasing configuration complexity (a)-(c); deviation of the $3p3h$ strength functions from the exact ones (d); $3p3h$ strength obtained on the IBM Quantum computers (e); $3p3h$ (exact) strength function profiles (f).

The two-dimensional heatmaps are shown on top of the panels to guide the eye. The even part of the Hamiltonian is mapped on three qubits constraining $\alpha_m = 3$ as the maximal configuration complexity. The increase of α_m gradually improves the description heading towards a clean LMG energy spectrum at $\alpha_m = 3$, which accurately reproduces the exact energies [47]. The same trend is seen in the strength functions, which at $\alpha_m < 3$ exhibit artificial peak structures causing decoherence at strong coupling and at $\alpha_m = 3$ reproduce the exact solution. The latter is illustrated in panel (c): both the $\alpha_m = 3$ and exact solutions trend toward the strength concentrated in a single peak at large \tilde{v} . This trend holds up to at least $\tilde{v} \sim 100$, and all the approaches satisfy the energy-weighted sum rule. Panel (d) illustrates the accuracy of the $\alpha_m = 3$ approach in terms of deviation from the exact strength functions: the median error and 90th percentile are $1.4 \cdot 10^{-9}$ and $3.5 \cdot 10^{-7}$, respectively. Hardware computation illustrated in panel (e) was performed on IBM Quantum devices using the optimized circuit [47] up to $\tilde{v} = 2$ and also showed the best quality of descrip-

tion at $\alpha_m = 3$.

At $\tilde{v} = 0$, all three approaches generate essentially identical spectra, which consist of three equidistant and equal-height peaks. With the increment of \tilde{v} , the levels repel, and the strength redistributes: the peak at $E = 0$ gradually grows while the others are suppressed. The inaccuracies of the $\alpha_m = \{1, 2\}$ approximations also increase with \tilde{v} , whereas the $\alpha_m = 3$ calculation demonstrates a clear picture of strength collectivization into a single dominant peak. In this way, we trace the emergence of collectivity via its gradual accumulation with the strengthening of interaction. Panel (f) of Fig. 3 shows the $S(E)$ profiles obtained from the $\alpha_m = 3$ simulation for each energy solution represented by separate curves, further clarifying the strength formation across the coupling regimes. One can distinguish, in particular, the two mechanisms of emerging collectivity: (i) the accumulation of the strength by a single transition at $E = 0$ due to its growing amplitude and (ii) the coherent contribution of multiple transitions.

In summary, we presented a microscopic approach to the response of strongly coupled fermionic systems with variable complexity of their quantum states. We showed that (i) the degree of complexity is a reliable classifier of the accuracy of the many-body approach with an established link to the exact theory, and (ii) accounting for emergent collectivity plays a critical role in obtaining spectroscopically accurate results. Our method demon-

strated that many-body correlations of growing complexity are efficiently generated if the emergent collectivity is utilized to order complex configurations in large ($N \approx 120$) systems. In particular, the GDR in ^{120}Sn is reproduced with nearly spectroscopic accuracy with correlated $2q \otimes 2\text{phonon}$ configurations. We argued that for nuclear spectral calculations, an efficient method of tackling configurations with varying complexity is the key ingredient, and such a method is accessible via quantum algorithms. The quantum EOM is implemented for the response of the LMG system, revealing a quantum benefit when building a hierarchy of approximations ordered by configuration complexity α_m due to the independence of the number of required quantum measurements on this parameter. Calculations on a digital simulator demonstrated the capability of qEOM to gradually approach the exact solution with growing α_m , efficiently accessing emergent collectivity via entanglement, which holds up to arbitrarily strong coupling. The available IBM Quantum hardware enables reliable computation up to the effective coupling strength of 1.0-1.5, which is in the range of nuclear structure physics. The method shows a reasonable scaling with the particle number, opening a new avenue to studies of nuclear and other strongly coupled many-body systems on quantum computers.

We acknowledge funding from US-NSF through the Grant PHY-2209376 and CAREER Grant PHY-1654379. We appreciate cloud access to IBM Quantum computers to run hardware calculations for this work.

-
- [1] P. C. Martin and J. S. Schwinger, Theory of many particle systems. 1., *Physical Review* **115**, 1342 (1959).
- [2] D. J. Rowe, Equations-of-Motion Method and the Extended Shell Model, *Review of Modern Physics* **40**, 153 (1968).
- [3] S. Adachi and P. Schuck, Landau's collision term in the memory function approach to the nuclear response function and the spreading width of giant resonances, *Nuclear Physics* **A496**, 485 (1989).
- [4] J. Dukelsky, G. Röpke, and P. Schuck, Generalized Brückner-Hartree-Fock theory and self-consistent RPA, *Nuclear Physics* **A628**, 17 (1998).
- [5] V. Olevano, J. Toulouse, and P. Schuck, A formally exact one-frequency-only Bethe-Salpeter-like equation. Similarities and differences between GW +BSE and self-consistent RPA, *Journal of Chemical Physics* **150**, 084112 (2019).
- [6] E. Litvinova and P. Schuck, Toward an accurate strongly-coupled many-body theory within the equation of motion framework, *Physical Review C* **100**, 064320 (2019).
- [7] P. Ring and P. Schuck, *The Nuclear Many-Body Problem* (Springer-Verlag Berlin Heidelberg, 1980).
- [8] E. Litvinova and Y. Zhang, Microscopic response theory for strongly coupled superfluid fermionic systems, *Physical Review C* **106**, 064316 (2022).
- [9] A. Bohr and B. R. Mottelson, *Nuclear structure*, Vol. 1 (World Scientific, 1969).
- [10] A. Bohr and B. R. Mottelson, *Nuclear structure*, Vol. 2 (Benjamin, New York, 1975).
- [11] D. Bes, R. Broglia, G. Dussel, R. Liotta, and R. Perazzo, On the many-body foundation of the nuclear field theory, *Nuclear Physics A* **260**, 77 (1976).
- [12] G. Bertsch, P. Bortignon, and R. Broglia, Damping of nuclear excitations, *Reviews of Modern Physics* **55**, 287 (1983).
- [13] F. Barranco, G. Potel, R. A. Broglia, and E. Vigezzi, Structure and reactions of ^{11}Be : many-body basis for single-neutron halo, *Physical Review Letters* **119**, 082501 (2017).
- [14] L. A. Malov and V. G. Soloviev, Fragmentation of single-particle states and neutron strength functions in deformed nuclei, *Nuclear Physics A* **270**, 87 (1976).
- [15] V. Soloviev, *Theory of Atomic Nuclei: Quasiparticles and Phonons* (Institute of Physics Publishing, 1992).
- [16] V. Tselyaev, Description of complex configurations in magic nuclei with the method of chronological decoupling of diagrams, *Soviet Journal of Nuclear Physics* **50**, 780 (1989).
- [17] S. P. Kamerdzhiev, G. Y. Tertychny, and V. I. Tselyaev, The method of time-ordered graph decoupling and its application to the description of giant resonances in magic nuclei, *Physics of Particles and Nuclei* **28**, 134 (1997).
- [18] E. Litvinova, P. Ring, and V. Tselyaev, Relativistic quasiparticle time blocking approximation: Dipole response of open-shell nuclei, *Physical Review C* **78**, 014312 (2008).

- [19] E. Litvinova, P. Ring, and V. Tselyaev, Mode coupling and the pygmy dipole resonance in a relativistic two-phonon model, *Physical Review Letters* **105**, 022502 (2010).
- [20] Y. Niu, Z. Niu, G. Colò, and E. Vigezzi, Particle-vibration coupling effect on the β decay of magic nuclei, *Physical Review Letters* **114**, 142501 (2015).
- [21] C. Robin and E. Litvinova, Time-reversed particle-vibration loops and nuclear Gamow-Teller response, *Physical Review Letters* **123**, 202501 (2019).
- [22] E. Litvinova, Relativistic approach to the nuclear breathing mode, *Physical Review C* **107**, L041302 (2023).
- [23] Z. Z. Li, Y. F. Niu, and G. Colò, Toward a unified description of isoscalar giant monopole resonances in a self-consistent quasiparticle-vibration coupling approach, *Physical Review Letters* **131**, 082501 (2023).
- [24] P. Papakonstantinou and R. Roth, Second random phase approximation and renormalized realistic interactions, *Physics Letters B* **671**, 356 (2009).
- [25] F. Knapp, N. Lo Iudice, P. Veselý, F. Andreozzi, G. De Gregorio, and A. Porrino, Dipole response in Sn132 within a self-consistent multiphonon approach, *Physical Review C* **90**, 014310 (2014).
- [26] F. Knapp, N. Lo Iudice, P. Veselý, F. Andreozzi, G. De Gregorio, and A. Porrino, Dipole response in 208Pb within a self-consistent multiphonon approach, *Physical Review C* **92**, 054315 (2015).
- [27] V. Yu. Ponomarev, Microscopic studies of two-phonon giant resonances, *Nuclear Physics A* **649**, 243 (1999).
- [28] N. Lo Iudice, V. Y. Ponomarev, C. Stoyanov, A. V. Sushkov, and V. V. Voronov, Low-energy nuclear spectroscopy in a microscopic multiphonon approach, *Journal of Physics G* **39**, 043101 (2012).
- [29] D. Savran *et al.*, Fragmentation and systematics of the pygmy dipole resonance in the stable N=82 isotones, *Physical Review C* **84**, 024326 (2011).
- [30] N. Tsoneva, M. Spieker, H. Lenske, and A. Zilges, Fine structure of the pygmy quadrupole resonance in $^{112,114}\text{Sn}$, *Nuclear Physics A* **990**, 183 (2019).
- [31] H. Lenske and N. Tsoneva, Dissolution of shell structures and the polarizability of dripline nuclei, *European Physical Journal A* **55**, 238 (2019).
- [32] D. Vretenar, A. V. Afanasjev, G. A. Lalazissis, and P. Ring, Relativistic hartree-bogoliubov theory: static and dynamic aspects of exotic nuclear structure, *Physics Reports* **409**, 101 (2005).
- [33] N. Paar, T. Nikšić, D. Vretenar, and P. Ring, Quasiparticle random phase approximation based on the relativistic Hartree-Bogolyubov model. 2. Nuclear spin and isospin excitations, *Physical Review C* **69**, 054303 (2004).
- [34] N. Paar, D. Vretenar, E. Khan, and G. Colò, Exotic modes of excitation in atomic nuclei far from stability, *Rep. Prog. Phys.* **70**, 691 (2007).
- [35] E. Litvinova, On the dynamical kernels of fermionic equations of motion in strongly-correlated media, *European Physical Journal A* **59**, 291 (2023).
- [36] P. J. Ollitrault, A. Kandala, C.-F. Chen, P. K. Barkoutsos, A. Mezzacapo, M. Pistoia, S. Sheldon, S. Woerner, J. M. Gambetta, and I. Tavernelli, Quantum equation of motion for computing molecular excitation energies on a noisy quantum processor, *Physical Review Research* **2**, 043140 (2020).
- [37] J. Rizzo, F. Libbi, F. Tacchino, P. J. Ollitrault, N. Marzari, and I. Tavernelli, One-particle green's functions from the quantum equation of motion algorithm, *Physical Review Research* **4**, 043011 (2022).
- [38] H. J. Lipkin, N. Meshkov, and A. Glick, Validity of many-body approximation methods for a solvable model:(i). exact solutions and perturbation theory, *Nuclear Physics B* **62**, 188 (1965).
- [39] D. S. Delion, P. Schuck, and J. Dukelsky, Self consistent random phase approximation and the restoration of symmetries within the three-level lipkin model, *Physical Review C* **72**, 064305 (2005).
- [40] P. Ribeiro, J. Vidal, and R. Mosseri, Thermodynamical limit of the lipkin-meshkov-glick model, *Phys. Rev. Lett.* **99**, 050402 (2007).
- [41] S. Lerma H. and J. Dukelsky, The Lipkin-Meshkov-Glick model as a particular limit of the SU(1,1) Richardson-Gaudin integrable models, *Nuclear Physics B* **870**, 421 (2013).
- [42] M. J. Cervia, A. B. Balantekin, S. N. Coppersmith, C. W. Johnson, P. J. Love, C. Poole, K. Robbins, and M. Saffman, Lipkin model on a quantum computer, *Physical Review C* **104**, 024305 (2021).
- [43] A. M. Romero, J. Engel, H. L. Tang, and S. E. Economou, Solving nuclear structure problems with the adaptive variational quantum algorithm, *Physical Review C* **105**, 064317 (2022).
- [44] M. Q. Hlatshwayo, Y. Zhang, H. Wibowo, R. LaRose, D. Lacroix, and E. Litvinova, Simulating excited states of the lipkin model on a quantum computer, *Physical Review C* **106**, 024319 (2022).
- [45] C. E. P. Robin and M. J. Savage, Quantum simulations in effective model spaces: Hamiltonian-learning variational quantum eigensolver using digital quantum computers and application to the lipkin-meshkov-glick model, *Physical Review C* **108**, 024313 (2023).
- [46] Y. Beaujeault-Taudiere and D. Lacroix, Solving the lipkin model using quantum computers with two qubits only with a hybrid quantum-classical technique based on the generator coordinate method, *Physical Review C* **109**, 024327 (2024).
- [47] M. Q. Hlatshwayo, J. Novak, and E. Litvinova, Quantum benefit of the quantum equation of motion for the strongly coupled many-body problem, *Physical Review C* **109**, 014306 (2024).
- [48] C. Popovici, P. Watson, and H. Reinhardt, Coulomb gauge confinement in the heavy quark limit, *Physical Review D* **81**, 105011 (2010).
- [49] S. Bassauer *et al.*, Electric and magnetic dipole strength in $^{112,114,116,118,120,122}\text{Sn}$, *Physical Review C* **102**, 034327 (2020).
- [50] G. Lalazissis, J. König, and P. Ring, *Physical Review C* **55**, 540 (1997).
- [51] V. I. Tselyaev, Subtraction method and stability condition in extended random-phase approximation theories, *Physical Review C* **88**, 054301 (2013).
- [52] E. F. Dumitrescu, A. J. McCaskey, G. Hagen, G. R. Jansen, T. D. Morris, T. Papenbrock, R. C. Pooser, D. J. Dean, and P. Lougovski, Cloud quantum computing of an atomic nucleus, *Physical Review Letters* **120**, 210501 (2018).
- [53] H.-H. Lu *et al.*, Simulations of subatomic many-body physics on a quantum frequency processor, *Physical Review A* **100**, 012320 (2019).
- [54] A. Roggero and J. Carlson, Dynamic linear response quantum algorithm, *Physical Review C* **100**, 034610

- (2019).
- [55] A. Roggero, C. Gu, A. Baroni, and T. Papenbrock, Preparation of excited states for nuclear dynamics on a quantum computer, *Physical Review C* **102**, 064624 (2020).
- [56] D. Lacroix, Symmetry-assisted preparation of entangled many-body states on a quantum computer, *Physical Review Letters* **125**, 230502 (2020).
- [57] E. A. Ruiz Guzman and D. Lacroix, Accessing ground-state and excited-state energies in a many-body system after symmetry restoration using quantum computers, *Physical Review C* **105**, 024324 (2022).
- [58] C. Robin, M. J. Savage, and N. Pillet, Entanglement rearrangement in self-consistent nuclear structure calculations, *Physical Review C* **103**, 034325 (2021).
- [59] D. Lacroix, E. A. Ruiz Guzman, and P. Siwach, Symmetry breaking/symmetry preserving circuits and symmetry restoration on quantum computers: A quantum many-body perspective, *European Physical Journal A* **59**, 3 (2023).
- [60] A. Asthana, A. Kumar, V. Abraham, H. Grimsley, Y. Zhang, L. Cincio, S. Tretiak, P. A. Dub, S. E. Economou, E. Barnes, and N. J. Mayhall, Quantum self-consistent equation-of-motion method for computing molecular excitation energies, ionization potentials, and electron affinities on a quantum computer, *Chemical Science* **14**, 2405 (2023).
- [61] J. Tilly *et al.*, The variational quantum eigensolver: A review of methods and best practices, *Physics Reports* **986**, 1 (2022).
- [62] T. Nakatsukasa, T. Inakura, and K. Yabana, Finite amplitude method for the solution of the random-phase approximation, *Physical Review C* **76**, 024318 (2007).
- [63] A. Bjelčić and T. Nikšić, Implementation of the quasiparticle finite amplitude method within the relativistic self-consistent mean-field framework: The program DIRQ-FAM, *Computer Physics Communications* **253**, 107184 (2020).